

Determinant-based Fast Greedy Sensor Selection Algorithm

Yuji Saito, Taku Nonomura, Keigo Yamada, Keisuke Asai
Tohoku University, Sendai, Miyagi 980-8579, Japan
 Yasuo Sasaki, and Daisuke Tsubakino
Nagoya University, Nagoya, Aichi, 464-8603, Japan

Abstract—The sparse sensor placement problem for the least square estimation is considered, by extending the previous novel approach in this paper. First, the objective function of the problem is redefined to be the maximization of the determinant of the matrix appearing in pseudo inverse matrix operations, leading to the maximization of the corresponding confidence intervals. The procedure for the maximization of the determinant of the corresponding matrix is proved to be the same as that of the previous QR method in the case of the number of sensors less than that of state variables. On the other hand, the authors have developed a new algorithm in the case of the number of sensors greater than that of state variables. Then, the unified formulation of both algorithms is derived, and the lower bound of the objective function given by this algorithm is shown using the monotone submodularity. In the proposed algorithm, optimal sensors are obtained by the QR method until the number of sensors is the same as that of the state variables, and, after that, new sensors are calculated by a proposed determinant-based greedy method which is accelerated by both determinant formula and matrix inversion lemma. The effectiveness of this algorithm on the dataset related to the global climate is demonstrated by comparing it with the results by other algorithms. The calculation results show that the computational time of the proposed extended determinant-based greedy algorithm is shorter than that of other methods with almost the minimum level of estimation errors.

Index Terms—Data processing, sensor placement, greedy algorithm.

I. INTRODUCTION

REDUCED-ORDER, modeling for fluid analysis and flow control gather a lot of attentions. A proper orthogonal decomposition (POD)[1], [2] is one of the effective methods to decompose the high-dimension data into several significant modes of flow fields. Here, POD is a data-driven method which gives us the most significant and relevant structure in the data, and it exactly corresponds to principal component analysis and Karhunen-Loeve (KL) decomposition, where the decomposed modes are orthogonal each other. The POD analysis for discrete data matrix can be carried out by applying the singular value decomposition, as is often the case in the

engineering fields. Although there are several advanced data-driven methods, dynamic mode decomposition[3], [4], empirical mode decomposition, and others which include efforts by the authors[5], [6], this research is only based on POD which is the most basic data-driven method for reduced-order modeling.

If the data, such as flow fields, can be effectively expressed by a limited number of POD modes, the limited sensor placed at appropriate positions gives us the approximated full state information. This effective observation might be one of the keys for flow control and flow prediction. This idea has been adopted by Manohar et al.[7], and the sparse-sensor-placement algorithm has been developed and discussed. The idea here is expressed by the following equation:

$$\begin{aligned} \mathbf{y} &= \mathbf{H}\mathbf{U}\mathbf{x} \\ &= \mathbf{C}\mathbf{x}. \end{aligned} \quad (1)$$

Here, $\mathbf{y} \in \mathbb{R}^p$, $\mathbf{x} \in \mathbb{R}^r$, $\mathbf{H} \in \mathbb{R}^{p \times n}$ and $\mathbf{U} \in \mathbb{R}^{n \times r}$ are the observation vector, the POD mode amplitude, the sparse sensor location matrix, and spatial POD modes, respectively. In addition, p , n , and r are numbers of sensor location, degrees of freedom of the spatial POD modes, and the rank for truncated POD, respectively. The problem above is considered to be one of the sensor selection problems when the POD mode \mathbf{U} and strength \mathbf{x} are assumed to be a sensor-candidate matrix and the latent state variables, respectively. The graphical image of the equation above is shown in Fig. 1.

The optimal sensor placement is an important challenge in the design, prediction, estimation, and control of high-dimensional systems. High-dimensional states can often leverage a latent low-dimensional representation, and this inherent compressibility enables sparse sensing. For example, in the applications of aerospace engineering, such as launch vehicles and satellites, the optimal sensor placement is an important subject in performance prediction, control of the system, fault diagnostics and prognostics, etc. because of the limitation of the installation, limitation of cost, and limitation of downlink capacity transferring measurement data. Therefore, the study on the optimal sensor placement is valuable in this field. Those sparse point sensors should be selected considering the POD modes. Although compressed sensing can recover a wider class of signals, the benefits of exploiting known patterns in data with optimized sensing is utilized, as similar to the previous study[7]. Drastic reductions in the required number of sensors and improved reconstruction can be expected in this

Assistant Professor, Department of Aerospace Engineering.
 Associate Professor, Department of Aerospace Engineering, also Presto, JST.

Graduate student, Department of Aerospace Engineering.
 Professor, Department of Aerospace Engineering.
 Graduate student, Department of Aerospace Engineering.
 Lecturer, Department of Aerospace Engineering.

case. In the series of studies, Clark et al. extended the idea and developed the optimization method placing sensors with a cost constraint[8]. Manohar et al. developed the sensor optimization method using the balance truncation for the linear system.[9]. Saito et al. extended the greedy method to vector sensor problems with considering the fluid dynamic measurement application.[10]

Thus far, this sensor selection problem has been solved by a convex approximation and a greedy algorithm, where the greedy algorithm was shown to be much faster than the convex approximation algorithms[7]. Table I summarizes a computational complexity based on each calculation methods: a brute-force searching, the convex approximation method, and the greedy algorithm, respectively. The previous study [7] introduced that the greedy algorithm is based on QR-discrete-empirical-interpolation method [11], [12] when the number of sensors is the same as that of state variables and its extension for the least square problem when the number of sensors is greater than that of state variables. Both convex approximation and greedy algorithm work pretty well for the sensor selection problem. The excellent idea of the QR method is extended in this study. When the number of sensors is greater than that of state variables, the theoretical background for calculation is not clear in the previous study in the greedy algorithm. Therefore, this paper introduces an improved formulation and presents its monotone submodularity and performance. In a new algorithm, optimal sensors are obtained by the QR method until the number of sensors is equal to state variables, and, after that, new sensors are calculated by a proposed determinant-based greedy method which is accelerated by both determinant formula and matrix inversion lemma.

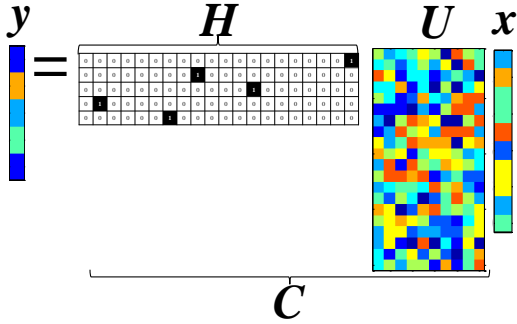


Fig. 1. Graphical image for sensor matrix H on (1)

TABLE I

COMPUTATIONAL COMPLEXITY OF EACH METHOD FOR SELECTING SENSORS[7].

Name	Computational complexity
Brute-force search	$\frac{n!}{(n-p)!p!} \sim O(n^p)$
Convex approximation method	$O(n^3)$ per iteration.
Greedy method	$p \leq r : O(nr^2)$ $p > r : O(n^3)$

II. ALGORITHM

A. Previous Greedy Algorithm for Sensors[7]

In the greedy algorithm based on QR decomposition for scalar measurement problem, i -th sensor is chosen where

$$i = \arg \max \|v_i\|_2^2. \quad (2)$$

Here, we initialize $v_i = [V_{i,1} \ V_{i,2} \ \dots \ V_{i,r}]$ and $\{V_{ij}\} = V = U$ and $\{V_{ij}\} = V = UU^T$ for $p = r$ and $p > r$ sensor conditions, respectively, as did in the previous study[7]. Given i index, the V matrix is pivoted and QR decomposed using newly selected v_i . After that, the next sensor is chosen for remaining matrix. The algorithms for $p = r$ and $p > r$ sensors are QR-discrete-empirical-interpolation method (QDEIM) and optimized sparse sensor placement as an extension of QDEIM, respectively.

The optimization is considered to conduct the maximization of determinant of the C matrix to stably solve x vector in the case of $p = r$. The selection of the sensor position is based on maximizing the norm of the corresponding row vector of the sensor-candidate matrix. On the other hand, the calculation algorithm for the condition $p > r$ has already been proposed in the previous study (which corresponds to the use of $V = UU^T$ instead of $V = U$), but, the validity of the algorithm has not been explained and clarified well in the previous study. The Gram-Schmidt algorithm equivalent to the previous QR algorithm is shown in Alg. 1.

Algorithm 1 Gram-Schmidt greedy algorithm for sparse sensor placement

```

Set sensor-candidate matrix  $U$ .
Set number of sensors  $p \geq r$ .
if  $p = r$  then
   $V = U$ 
else if  $p > r$  then
   $V = UU^T$ 
end if
for  $k = 1, \dots, p$  do
   $v_i = [V_{i1} \ V_{i2} \ \dots \ V_{ir}]$ 
   $i \leftarrow \arg \max \|v_i\|_2^2$ 
   $w_k \leftarrow v_i^i$ 
   $V \leftarrow V - Vw_k^T w_k / \|w_k\|_2^2$ 
   $H_{k,i} = 1$ 
end for

```

B. Proposed Determinant-based Greedy Algorithm

Let C_k denotes k th sensor-candidate matrix as follows:

$$C_k = [u_{i_1}^T \ u_{i_2}^T \ \dots \ u_{i_{k-1}}^T \ u_{i_k}^T]^T, \quad (3)$$

where i_k and u_{i_k} are an index of the k th selected sensor and the corresponding row vector of the sensor-candidate matrix. The following algorithm can be derived straightforwardly by considering the pseudo inverse matrix of C . The greedy sensor-selection problem is defined as the locations of first-to- $(k-1)$ th

sensors selected thus far are known. Equation 1 can be solved as $\mathbf{x} = \mathbf{C}^+ \mathbf{y}$ and divided into two cases:

$$\mathbf{x} = \begin{cases} \mathbf{C}^T (\mathbf{C} \mathbf{C}^T)^{-1} \mathbf{y}, & p \leq r, \\ (\mathbf{C}^T \mathbf{C})^{-1} \mathbf{C}^T \mathbf{y}, & p > r. \end{cases} \quad (4)$$

Here, \mathbf{C} is assumed to be a column-full-rank or row-full-rank matrix. Therefore, the optimization could also be divided into two cases: the maximization of determinant of $\mathbf{C} \mathbf{C}^T$ and $\mathbf{C}^T \mathbf{C}$ in the cases of $p \leq r$ and $p > r$, respectively. The sensors up to $k-1$ are already selected and it becomes the sensor selecting problem only k in the greedy algorithm. The subject is expressed as Algorithm 2 summarizes. The problem in the case of $k \leq r$ has been conducted by Manohar et al. [9]. Their algorithm selects the sensor position based on maximizing the norm of the corresponding row vector of the sensor-candidate matrix \mathbf{U} applying the QR decomposition, as explained before. Although they explained in [9] that the QR decomposition provides an approximate greedy solution for the maximization of the determinant of \mathbf{C} , to the best of our knowledge, they have yet to explain this mathematical background in detail. Therefore, the mathematical background for the maximization of determinant of $\mathbf{C} \mathbf{C}^T$ will be described in the next section. The problem in the case of $k > r$ has been conducted in previous studies [13] [14], and the proposed objective function in this study (the maximization of determinant of $\mathbf{C}^T \mathbf{C}$) corresponds to designing the experiment to minimize the volume of the resulting confidence ellipsoid[13].

Algorithm 2 Determinant-based greedy algorithm for sparse sensor placement

```

for  $k = 1, \dots, r, \dots, p$  do
  if  $k = 1$  then
     $i_k = \arg \max \mathbf{u}_i \mathbf{u}_i^T$ 
  else if  $k \leq r$  then
     $i_k = \arg \max \det(\mathbf{C}_k \mathbf{C}_k^T)$ 
     $= \arg \max \det \left( \begin{bmatrix} \mathbf{C}_{k-1} \\ \mathbf{u}_i \end{bmatrix} \begin{bmatrix} \mathbf{C}_{k-1}^T & \mathbf{u}_i^T \end{bmatrix} \right)$ 
  else
     $i_k = \arg \max \det(\mathbf{C}_k^T \mathbf{C}_k)$ 
     $= \arg \max \det \left( \begin{bmatrix} \mathbf{C}_{k-1}^T & \mathbf{u}_i^T \end{bmatrix} \begin{bmatrix} \mathbf{C}_{k-1} \\ \mathbf{u}_i \end{bmatrix} \right)$ 
  end if
  Set sensor-candidate matrix
   $\mathbf{C}_k = [ \mathbf{u}_{i_1}^T \quad \mathbf{u}_{i_2}^T \quad \dots \quad \mathbf{u}_{i_{k-1}}^T \quad \mathbf{u}_{i_k}^T ]^T$ 
end for

```

The step-by-step maximization of the determinant of $\mathbf{C}_k \mathbf{C}_k^T$ is considered using the greedy method in the case of $k \leq r$. This objective is the maximization of the determinant of the matrix appearing in pseudo inverse matrix operations, leading to the maximization of confidence intervals. It can be expanded

as follows (see, e.g., [15] for detailed derivation):

$$\begin{aligned} \det(\mathbf{C}_k \mathbf{C}_k^T) &= \det \left(\begin{bmatrix} \mathbf{C}_{k-1} \\ \mathbf{u}_i \end{bmatrix} \begin{bmatrix} \mathbf{C}_{k-1}^T & \mathbf{u}_i^T \end{bmatrix} \right) \\ &= \det \left(\begin{bmatrix} \mathbf{C}_{k-1} \mathbf{C}_{k-1}^T & \mathbf{C}_{k-1} \mathbf{u}_i^T \\ \mathbf{u}_i \mathbf{C}_{k-1}^T & \mathbf{u}_i \mathbf{u}_i^T \end{bmatrix} \right) \\ &= \mathbf{u}_i \left(\mathbf{I} - \mathbf{C}_{k-1}^T (\mathbf{C}_{k-1} \mathbf{C}_{k-1}^T)^{-1} \mathbf{C}_{k-1} \right) \mathbf{u}_i^T \\ &\quad \times \det(\mathbf{C}_{k-1} \mathbf{C}_{k-1}^T), \end{aligned} \quad (5)$$

and, therefore,

$$\begin{aligned} &\arg \max \det(\mathbf{C}_k \mathbf{C}_k^T) \\ &= \arg \max \mathbf{u}_i \left(\mathbf{I} - \mathbf{C}_{k-1}^T (\mathbf{C}_{k-1} \mathbf{C}_{k-1}^T)^{-1} \mathbf{C}_{k-1} \right) \mathbf{u}_i^T. \end{aligned} \quad (6)$$

In the k th step of sensor selection of the previous QR (or Gram-Schmidt) method and the present method, the following equality is obtained:

$$\mathbf{v}_i \mathbf{v}_i^T = \mathbf{u}_i \left(\mathbf{I} - \mathbf{C}_{k-1}^T (\mathbf{C}_{k-1} \mathbf{C}_{k-1}^T)^{-1} \mathbf{C}_{k-1} \right) \mathbf{u}_i^T, \quad (7)$$

and, therefore, both algorithms are equivalent [7]. This is because $\mathbf{I} - \mathbf{C}_{k-1}^T (\mathbf{C}_{k-1} \mathbf{C}_{k-1}^T)^{-1} \mathbf{C}_{k-1} = \mathbf{P}_{\mathbf{C}_{k-1}}^\perp$ is the projection matrix to the orthogonal complement space against the already selected sensor vector space, and therefore the absolute value of sensor-candidate matrix in the orthogonal complement space $\mathbf{u}_i \left(\mathbf{I} - \mathbf{C}_{k-1}^T (\mathbf{C}_{k-1} \mathbf{C}_{k-1}^T)^{-1} \mathbf{C}_{k-1} \right) \mathbf{u}_i^T$ exactly corresponds to the absolute value of \mathbf{v}_i which is the sensor-candidate vector subtracted by the already selected sensor components in the k th step. See in Appendix for the detailed proof.

Although an efficient way to recursively calculate $(\mathbf{C}_k \mathbf{C}_k^T)^{-1}$ is derived when the new sensor is found and the step number k is incremented, as follows:

$$\begin{aligned} (\mathbf{C}_k \mathbf{C}_k^T)^{-1} &= \left(\begin{bmatrix} \mathbf{C}_{k-1} \\ \mathbf{u}_{i_k} \end{bmatrix} \begin{bmatrix} \mathbf{C}_{k-1}^T & \mathbf{u}_{i_k}^T \end{bmatrix} \right)^{-1} \\ &= \begin{pmatrix} \mathbf{A} & \mathbf{b}^T \\ \mathbf{b} & d \end{pmatrix}, \end{aligned} \quad (8)$$

where

$$\begin{aligned} \mathbf{A} &= (\mathbf{C}_{k-1} \mathbf{C}_{k-1}^T)^{-1} \\ &\quad \left\{ \mathbf{I} + \frac{\mathbf{C}_{k-1} \mathbf{u}_{i_k}^T \mathbf{u}_{i_k} \mathbf{C}_{k-1}^T (\mathbf{C}_{k-1} \mathbf{C}_{k-1}^T)^{-1}}{\mathbf{u}_{i_k} \left(\mathbf{I} - \mathbf{C}_{k-1}^T (\mathbf{C}_{k-1} \mathbf{C}_{k-1}^T)^{-1} \mathbf{C}_{k-1} \right) \mathbf{u}_{i_k}^T} \right\}, \\ \mathbf{b} &= \frac{-\mathbf{u}_{i_k} \mathbf{C}_{k-1}^T (\mathbf{C}_{k-1} \mathbf{C}_{k-1}^T)^{-1}}{\mathbf{u}_{i_k} \left(\mathbf{I} - \mathbf{C}_{k-1}^T (\mathbf{C}_{k-1} \mathbf{C}_{k-1}^T)^{-1} \mathbf{C}_{k-1} \right) \mathbf{u}_{i_k}^T}, \\ d &= \frac{1}{\mathbf{u}_{i_k} \left(\mathbf{I} - \mathbf{C}_{k-1}^T (\mathbf{C}_{k-1} \mathbf{C}_{k-1}^T)^{-1} \mathbf{C}_{k-1} \right) \mathbf{u}_{i_k}^T}, \end{aligned}$$

the total computational speed of the previous QR method is faster than that of the greedy algorithm and the previous QR method is generally chosen for this former part in the condition of $k < r$ except for the validation in the this paper. This algorithm is not straightforwardly used for the practical applications, but the algorithm is described in Alg. 3.

Algorithm 3 Determinant-based greedy algorithm for sparse sensor placement for $k \leq r$ (corresponds to the previous QR algorithm of $p = r$)

Set sensor-candidate matrix U .
 $\mathbf{u}_i = [U_{i,1} \ U_{i,2} \ \dots \ U_{i,r}]$
 $i \leftarrow \arg \max (1 + \mathbf{u}_i \mathbf{u}_i^T)$
 $H_{1,i} = 1$
 $\mathbf{C} = \mathbf{u}_i$
 $[U_{i,1} \ U_{i,2} \ \dots \ U_{i,r}] \leftarrow [0, 0, \dots, 0]$
for $k = 2, \dots, r$ **do**
 $\mathbf{u}_i = [U_{i,1} \ U_{i,2} \ \dots \ U_{i,r}]$
 $i \leftarrow \arg \max_i \mathbf{u}_i \left(\mathbf{I} - \mathbf{C}^T (\mathbf{C} \mathbf{C}^T)^{-1} \mathbf{C} \right) \mathbf{u}_i^T$
 Update $(\mathbf{C} \mathbf{C}^T)^{-1}$ using (8)
 $H_{k,i} = 1$
 $[U_{i,1} \ U_{i,2} \ \dots \ U_{i,r}] \leftarrow [0, 0, \dots, 0]$
end for

The maximization of the determinant of $\mathbf{C}^T \mathbf{C}$ is simply considered in the case of $k \geq r$ (see, e.g., [15] for detailed derivation.).

$$\begin{aligned} \det(\mathbf{C}_k^T \mathbf{C}_k) &= \det \left(\begin{bmatrix} \mathbf{C}_{k-1}^T & \mathbf{u}_i^T \end{bmatrix} \begin{bmatrix} \mathbf{C}_{k-1} \\ \mathbf{u}_i \end{bmatrix} \right) \\ &= \left(1 + \mathbf{u}_i (\mathbf{C}_{k-1}^T \mathbf{C}_{k-1})^{-1} \mathbf{u}_i^T \right) \det(\mathbf{C}_{k-1}^T \mathbf{C}_{k-1}). \end{aligned} \quad (9)$$

Therefore,

$$\begin{aligned} i &= \arg \max_i \det(\mathbf{C}_{k-1}^T \mathbf{C}_{k-1} + \mathbf{u}_i^T \mathbf{u}_i) \\ &= \arg \max_i \left(1 + \mathbf{u}_i (\mathbf{C}_{k-1}^T \mathbf{C}_{k-1})^{-1} \mathbf{u}_i^T \right). \end{aligned} \quad (10)$$

The complexity of this procedure is only $O(r^2)$ for one candidate sensor vector when inverse $(\mathbf{C}_{k-1}^T \mathbf{C}_{k-1})^{-1}$ is known, and the complexity when searching all components of vector becomes $O(nr^2)$. The inverse $(\mathbf{C}_k^T \mathbf{C}_k)^{-1}$ can be computed recursively using the matrix inversion lemma when the new sensor is found and the step number k is incremented, as follows:

$$\begin{aligned} &(\mathbf{C}_k^T \mathbf{C}_k)^{-1} \\ &= (\mathbf{C}_{k-1}^T \mathbf{C}_{k-1} + \mathbf{u}_i^T \mathbf{u}_i)^{-1} \\ &= (\mathbf{C}_{k-1}^T \mathbf{C}_{k-1})^{-1} \\ &\quad \left(\mathbf{I} - \mathbf{u}_i^T \left(1 + \mathbf{u}_i (\mathbf{C}_{k-1}^T \mathbf{C}_{k-1})^{-1} \mathbf{u}_i^T \right)^{-1} \mathbf{u}_i (\mathbf{C}_{k-1}^T \mathbf{C}_{k-1})^{-1} \right). \end{aligned} \quad (11)$$

C. Unified Expression for Proposed Algorithm

Here, we introduce the unified expressions for both cases in which the number of sensors is less than that of the modes and the number of sensors is greater than or equal to that of the modes. The maximization of the term $\det(\mathbf{C}^T \mathbf{C} + \epsilon \mathbf{I})$ is considered in this case, where ϵ is a sufficiently small number. This objective function is approximately corresponding to $\det(\mathbf{C}^T \mathbf{C})$ when the number of sensors is greater than or equal

Algorithm 4 Determinant-based greedy algorithm for sparse sensor placement for $k > r$

Set sensor-candidate matrix U .
 Obtain \mathbf{H}_0 using the previous QR algorithm (or Alg. 3) for the number of sensors $p_0 = r$.
 Set $(\mathbf{C}^T \mathbf{C})^{-1} = (\mathbf{U}^T \mathbf{H}_0^T \mathbf{H}_0 \mathbf{U})^{-1}$
for i of sensor position chosen by conventional greedy algorithm **do**
 Set $\mathbf{U}_i = [U_{i,1} \ U_{i,2} \ \dots \ U_{i,r}] = [0, 0, \dots, 0]$
end for
for $k = p_0 + 1, \dots, p$ **do**
 $\mathbf{U}_i = [U_{i,1} \ U_{i,2} \ \dots \ U_{i,r}]$
 $i \leftarrow \arg \max (1 + \mathbf{u}_i (\mathbf{C}^T \mathbf{C})^{-1} \mathbf{u}_i)$
 $(\mathbf{C}^T \mathbf{C})^{-1}$
 $\leftarrow (\mathbf{C}^T \mathbf{C})^{-1} \left(\mathbf{I} - \mathbf{u}_i^T \left(1 + \mathbf{u}_i (\mathbf{C}^T \mathbf{C})^{-1} \mathbf{u}_i^T \right)^{-1} \mathbf{u}_i (\mathbf{C}^T \mathbf{C})^{-1} \right)$
 $H_{k,i} = 1$
 $[U_{i,1} \ U_{i,2} \ \dots \ U_{i,r}] \leftarrow [0, 0, \dots, 0]$
end for

to that of the modes. On the other hand, when the number of sensors p is less than that of the modes r , it becomes

$$\begin{aligned} \det(\mathbf{C}^T \mathbf{C} + \epsilon \mathbf{I}) &= \epsilon^r \det \left(\mathbf{I} + \frac{1}{\epsilon} \mathbf{C}^T \mathbf{C} \right) \\ &= \epsilon^r \det \left(\mathbf{I} + \frac{1}{\epsilon} \mathbf{C} \mathbf{C}^T \right) \\ &= \epsilon^{r-p} \det(\mathbf{C} \mathbf{C}^T + \epsilon \mathbf{I}), \end{aligned} \quad (12)$$

and then the objective function corresponds to the maximization of $\det(\mathbf{C} \mathbf{C}^T + \epsilon \mathbf{I}) \sim \det(\mathbf{C} \mathbf{C}^T)$ as we did in the previous subsection. Therefore, the approximated objective function is defined to be $\det(\mathbf{C}^T \mathbf{C} + \epsilon \mathbf{I})$ which asymptotically approaches to the maximization of the determinant in the limit that ϵ goes to 0. Although this function should not be implemented in the computational code because it may include large round-off error when ϵ is sufficiently small to neglect its effects, this approximated function will be used for the proof of submodularity and discussion of the approximation rate in the next session.

III. SUBMODULAR FUNCTIONAL AND APPROXIMATION RATE

The objective function $f(S) = \log \det(\mathbf{C}_S^T \mathbf{C}_S + \epsilon \mathbf{I})$ is proved to be the monotone submodular function and then the approximation rate of the greedy algorithm is discussed in this section, where S is defined to be a sensor set. The two sensor sets S and T are considered, and the set S is assumed to be a subset of T :

$$S \subset T. \quad (13)$$

In this condition, the submodular function is defined as follows:

$$f(S \cup \{i\}) - f(S) \geq f(T \cup \{i\}) - f(T), \quad (14)$$

where i is an arbitrary element which satisfies $i \in V \setminus T$. Here, V is defined to be a set of all possible sensor candidates.

$f(S) = \log \det(\mathbf{C}_S^T \mathbf{C}_S + \epsilon \mathbf{I})$ becomes a submodular monotone function as shown here.

Theorem III.1. *The function $f(S) = \log \det(\mathbf{C}_S^T \mathbf{C}_S + \epsilon \mathbf{I})$ is submodular, where \mathbf{C}_S^T is a sensor matrix of set S .*

Proof: The \mathbf{C} matrices of sensor sets S and T are denoted to be \mathbf{C}_S and \mathbf{C}_T , respectively.

$$\begin{aligned} f(S \cup \{i\}) - f(S) &= \log \det(\mathbf{C}_S^T \mathbf{C}_S + \mathbf{u}_i^T \mathbf{u}_i + \epsilon \mathbf{I}) - \log \det(\mathbf{C}_S^T \mathbf{C}_S + \epsilon \mathbf{I}) \\ &= \log \det\left(\left(\mathbf{C}_S^T \mathbf{C}_S + \mathbf{u}_i^T \mathbf{u}_i + \epsilon \mathbf{I}\right)\left(\mathbf{C}_S^T \mathbf{C}_S + \epsilon \mathbf{I}\right)^{-1}\right) \\ &= \log \det\left(\mathbf{I} + \mathbf{u}_i^T \mathbf{u}_i \left(\mathbf{C}_S^T \mathbf{C}_S + \epsilon \mathbf{I}\right)^{-1}\right) \\ &= \log\left(1 + \mathbf{u}_i \left(\mathbf{C}_S^T \mathbf{C}_S + \epsilon \mathbf{I}\right)^{-1} \mathbf{u}_i^T\right) \end{aligned} \quad (15)$$

and

$$\begin{aligned} f(T \cup \{i\}) - f(T) &= \log \det\left(1 + \mathbf{u}_i \left(\mathbf{C}_T^T \mathbf{C}_T + \epsilon \mathbf{I}\right)^{-1} \mathbf{u}_i^T\right) \\ &= \log \det\left(1 + \mathbf{u}_i \left(\mathbf{C}_S^T \mathbf{C}_S + \mathbf{C}_{T \setminus S}^T \mathbf{C}_{T \setminus S} + \epsilon \mathbf{I}\right)^{-1} \mathbf{u}_i^T\right) \\ &= \log \det\left(1 + \mathbf{u}_i \left(\mathbf{C}_S^T \mathbf{C}_S + \epsilon \mathbf{I}\right)^{-1}\right. \\ &\quad \left.\left(\mathbf{I} - \mathbf{C}_{T \setminus S}^T \left(\mathbf{I} + \mathbf{C}_{T \setminus S} \left(\mathbf{C}_S^T \mathbf{C}_S + \epsilon \mathbf{I}\right)^{-1} \mathbf{C}_{T \setminus S}^T\right)^{-1}\right.\right. \\ &\quad \left.\left.\mathbf{C}_{T \setminus S} \left(\mathbf{C}_S^T \mathbf{C}_S + \epsilon \mathbf{I}\right)^{-1} \mathbf{u}_i^T\right)\right) \\ &= \log \det\left(1 + \mathbf{u}_i \left(\mathbf{C}_S^T \mathbf{C}_S + \epsilon \mathbf{I}\right)^{-1} \mathbf{u}_i^T\right. \\ &\quad \left.- \mathbf{u}_i \left(\mathbf{C}_S^T \mathbf{C}_S + \epsilon \mathbf{I}\right)^{-1} \mathbf{C}_{T \setminus S}^T\right. \\ &\quad \left.\left(\mathbf{I} + \mathbf{C}_{T \setminus S} \left(\mathbf{C}_S^T \mathbf{C}_S + \epsilon \mathbf{I}\right)^{-1} \mathbf{C}_{T \setminus S}^T\right)^{-1}\right. \\ &\quad \left.\mathbf{C}_{T \setminus S} \left(\mathbf{C}_S^T \mathbf{C}_S + \epsilon \mathbf{I}\right)^{-1} \mathbf{u}_i^T\right). \end{aligned} \quad (16)$$

The second terms in (15) and (16) are always positive and the last term in the logarithm of (16) is always non-positive because the matrix inside between \mathbf{u}_i and \mathbf{u}_i^T is symmetric and the corresponding quadratic forms should be always positive and non-negative, respectively. Comparing terms inside the logarithm in (15) and (16), we get

$$f(S \cup \{i\}) - f(S) \geq f(T \cup \{i\}) - f(T), \quad (17)$$

and f is a submodular function. ■

Theorem III.2. *The function f is monotone.*

Proof: Consider an arbitrary set S and an arbitrary element $i \in V \setminus S$. In this case,

$$\begin{aligned} f(S \cup \{i\}) &= \log \det(\mathbf{C}_S^T \mathbf{C}_S + \mathbf{u}_i^T \mathbf{u}_i + \epsilon \mathbf{I}) \\ &= \log \det(\mathbf{C}_S^T \mathbf{C}_S + \epsilon \mathbf{I}) + \log \det\left(\mathbf{I} + \mathbf{u}_i^T \mathbf{u}_i \left(\mathbf{C}_S^T \mathbf{C}_S + \epsilon \mathbf{I}\right)^{-1}\right) \\ &= f(S) + \log\left(1 + \mathbf{u}_i \left(\mathbf{C}_S^T \mathbf{C}_S + \epsilon \mathbf{I}\right)^{-1} \mathbf{u}_i^T\right). \end{aligned} \quad (18)$$

Here, $\log\left(1 + \mathbf{u}_i \left(\mathbf{C}_S^T \mathbf{C}_S + \epsilon \mathbf{I}\right)^{-1} \mathbf{u}_i^T\right) > 0$ because the matrix of the quadratic form is symmetric and then it is nonnegative. Therefore,

$$f(S \cup \{i\}) > f(S), \quad (19)$$

and f is monotone submodular. ■

Therefore, the following inequality proved by Nemhauser et al. can be applied to the monotone submodular function[16].

$$\left(1 - \left(1 - \frac{1}{k}\right)\right)^k f(S_{\text{opt}}) \leq f(S_{\text{greedy}}). \quad (20)$$

Here, k denotes the number of sensors, $S_{\text{opt}} \in V$ is an optimum solution, and $S_{\text{greedy}} \in V$ is the solution obtained by the greedy algorithm including the present formulation. Here, the factor $\alpha_k = \left(1 - \left(1 - \frac{1}{k}\right)\right)^k$ is monotonically decreasing and approaches to $1 - 1/e \sim 0.63$, when $k \rightarrow \infty$. Therefore,

$$0.63f(S_{\text{opt}}) \leq f(S_{\text{greedy}}), \quad (21)$$

and this provides the lower bounds of the greedy approximation.

IV. RESULTS AND DISCUSSIONS

The numerical experiments are conducted and the proposed methods are validated. Hereinafter, three different implementations of the greedy methods are compared: QR, DG, and QD methods listed in Table II. Here, the QR method is the greedy method proposed in the previous study[7], the DG method is the greedy method for the pure maximization of the determinant, and the QD method is the greedy method, the former part of which is replaced by the QR method which is mathematically proved to be the equivalent algorithm to the greedy method for the pure maximization of the determinant. Table III explains the computational complexities of each method for selecting p sensors. The QD method is introduced because the QR implementation for the former greedy optimization is much faster than the DG method, and both implementations are demonstrated to give us the same numerical optimized solution without being disturbed by round-off errors in the practical situations. A random selection and the convex approximation method[14] are evaluated as the references in addition to greedy methods.

TABLE II
GREEDY SENSOR SELECTION METHODS INVESTIGATED IN THE THIS STUDY

Name	Method	Implementation
QR[7]	$p \leq r$: QR for \mathbf{C}	Alg. 1
	$p > r$: QR for $\mathbf{C}\mathbf{C}^T$	Alg. 1
DG (present) ^a	$p \leq r$: arg max det($\mathbf{C}\mathbf{C}^T$)	Alg. 3 (Alg. 2)
	$p > r$: arg max det($\mathbf{C}^T\mathbf{C}$)	Alg. 4 (Alg. 2)
QD (present, recommended) ^a	$p \leq r$: QR for \mathbf{C}	Alg. 1 (Alg. 2)
	$p > r$: arg max det($\mathbf{C}^T\mathbf{C}$)	Alg. 4 (Alg. 2)

^a Both DG and QD methods are mathematically equivalent algorithms as proved in this paper.

TABLE III

COMPUTATIONAL COMPLEXITIES OF EACH METHOD FOR SELECTING p TH SENSORS.

Name	Computational complexity
QR[7]	$p \leq r : O(nr^2)$ $p > r : O(n^3)$
DG(present)	$p \leq r : O(pnr^2)$ $p > r : O(pnr^2)$
QD(present, recommended)	$p \leq r : O(pnr)$ $p > r : O(pnr^2)$
convex[14]	$O(n^3)$ per iterations *usually converges around 100 iterations.

TABLE IV

COMPUTATIONAL ENVIRONMENTS

Processor information	Intel(R) Core(TM) i7-6800K@ 3.40 GHz
Random access memory	128 GB
System type	64 bit operating system x64 base processor
Program code	Matlab R2013a [17]
Operating system	Windows 10 Pro Version:1890

A. Random sensor problem

The random sensor-candidate matrices, $U \in \mathbb{R}^{2000 \times r}$, were set, where the component of the matrices is given by the Gaussian distribution of $\mathcal{N}(0, 1)$ in this validation. The random selection, convex approximation, QR, DG and QD methods listed in Table II are evaluated. The determinant of $CC^T = HUU^T H^T$ ($p \leq r$) and $C^T C = U^T H^T H U$ ($p > r$) are calculated using both sensor-candidate matrices after selecting sensors. The random sensor problem is conducted under the computational environments as listed in Table IV. Fig. 2 shows the relationship between the determinant of CC^T ($p \leq r$) or $C^T C$ ($p > r$) and a number of sensors, p in POD mode $r = 10$ for the random sensor problem, obtained by the random selection (a black solid line with close circle), convex approximation (a blue solid line with close circle), QR (a red solid line with close circle), DG (a black dot line with open circle), and QD (a gray solid line with close circle) methods. All plots are normalized by the determinant of CC^T ($p \leq r$) or $C^T C$ ($p > r$) of the QR method. The normalized determinants of CC^T of both DG and QD methods are the same as that of the QR method in the case of $p \leq r$, and we can confirm what is shown in the previous theoretical procedure. On the other hand, the normalized determinants of $C^T C$ of both QR and QD methods increase as the number of sensors increases in the case of $p > r$. Although the computational complexity or time of the convex approximation method is much larger than those of other calculation methods, the convex approximation method obtains the highest normalized determinant of $C^T C$ in $p > 15$ in all methods. Fig. 3 shows the relationship the computational time and the number of sensors, p in POD mode $r = 10$ for the random sensor problem. Table III explains that the computational complexity of the

convex approximation algorithm is the largest in all calculation methods. The computational complexity of the QR method is close to that of the convex approximation method because the QR method is implemented in Matlab using the native Matlab "qr()" subroutine and return the desired list of all sensors. The computational times of the QR and QD methods in $p \leq r$ are the same as each other because the same algorithm is used in this case. The computational time of the DG method gradually increases as the number of sensors increases because a sensor is chosen by using the step-by-step maximization of the determinant of $C_k C_k^T$ or $C_k^T C_k$ is considered. On the other hand, the computational time for the QR method is almost constant in $1 \leq p \leq 10$ and $11 \leq p \leq 20$, respectively, because it takes a long time to conduct the full QR decomposition. The computational time of the QR method rapidly increases at $p = 11$ because the dimension of the matrix processed by the QR decomposition increases from $U \in \mathbb{R}^{n \times r}$ to $UU^T \in \mathbb{R}^{n \times n}$. The trend of the computational time for the QD method is similar to that for the QR method, but, the computational time of the QD method is much shorter than that of the QR method in the case of $p > r$. Therefore, the QD method proposed in this paper is more effective for sparse sensor placement than the convex algorithm because the determinant of CC^T ($p \leq r$) and $C^T C$ ($p > r$) is larger and the computational time of the QD method is much shorter than that of other calculation methods in the case of $1 \leq p \leq 20$ (POD mode $r : 10$) for the random sensor problem.

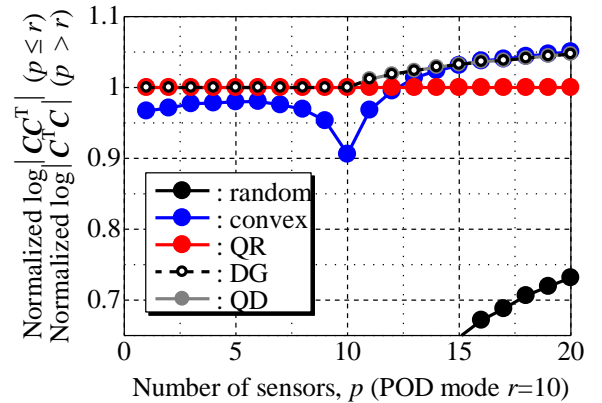


Fig. 2. Normalized by the determinant of CC^T ($p \leq r$) or $C^T C$ ($p > r$) vs. number of sensors in POD mode $r = 10$ for random sensor problem

B. NOAA-SST

A data set that we adopt is the NOAA OISST (NOAA-SST) V2 mean sea surface temperature set, comprising weekly global sea surface temperature measurements in the years between 1990 and 2000[18]. There are a total of 520 snapshots on a 360×180 spatial grid (Fig. 4). The sparse sensor problem for NOAA-SST is also conducted under the computational environments as listed in Table IV, similar to the former random sensor problem. Fig. 5 shows the relationship between the estimation error and the number of POD modes, where the estimation error is defined to be the ratio of the difference between the reconstructed data and the full observation data

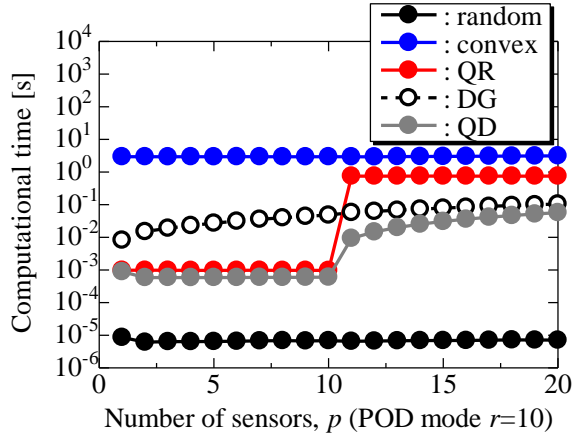


Fig. 3. Computational time vs. number of sensors in POD mode $r = 10$ for random sensor problem

to the full observation. In the case of NOAA-SST, the POD modes are truncated and the $r = 10$ low-dimensional representation are obtained. Fig. 5 shows the minimum estimation error is 0.30 in $r = 10$. We consider the results of the sensor selection problem (The number of sensors, $p : 1 - 20$) solved by each method; the random selection, the convex approximation[14], QR[7], DG and QD methods listed in Table II. Fig. 6 shows the sensor positions selected by the random selection, the convex approximation method, the QR and QD methods, respectively in the case of $r = p = 10$. Note that all sensors of the QD method are located at the same position as those of the DG method in all cases as well as in the previous random sensor problem.

Fig. 7 shows the relationship between the estimation error and the number of sensors in POD mode $r = 10$ for NOAA-SST problem. All estimation errors decrease as the number of sensors increases. Three estimation errors of the QR, DG and QD methods coincide with each other because all sensor locations are the same as each other in the case of $p = 10$. The estimation errors of both DG and QD methods are also the same as each other in the case of $p > r$ as well as in the random sensor problem. Although the estimation error of QR also decreases as the number of sensors increases, better sensor positions cannot be selected using the QR method than using the DG or QD method. Therefore, both DG and QD methods in the case of $p > r$ are more accurate sensor selection methods than the QR method in which the QR decomposition of UU^T is conducted. Fig. 8 shows the computational time of each method for selecting sensors in each condition. Although the trend in Fig. 8 is the same as that in Fig. 3, it is noticeable that the computational time of the convex approximation method is approximately three hours. On the other hand, the computational time of the QD method is just a few seconds with a lower estimation error. These results show that the proposed method, which is called the QD method in this paper, is a more efficient method combining the best properties of shorter computational time and more high accuracy sensor selection in the conditions in which the numbers of sensors and POD modes are $p = 1 - 20$ and $r = 10$, respectively.

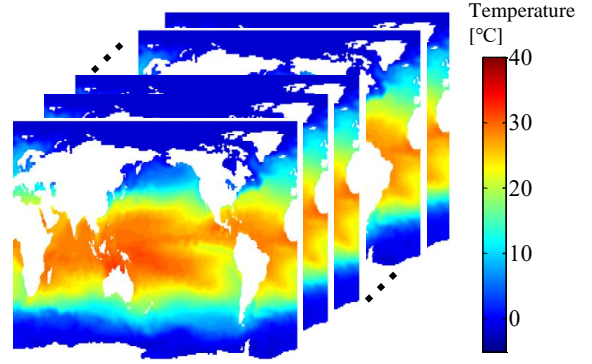


Fig. 4. Data set

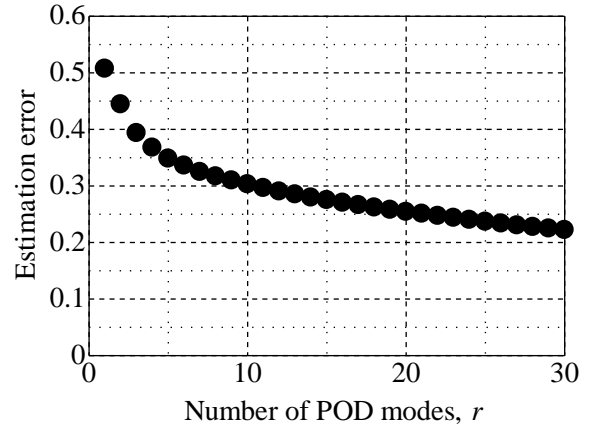


Fig. 5. Estimation error vs. number of POD modes for NOAA-SST problem

V. CONCLUSIONS

The sparse sensor placement problem is considered for the least square estimation. First, the objective function of the problem is redefined to be the maximization of the determinant of the matrix appearing in pseudo inverse matrix operations, leading to the maximization of the corresponding confidence intervals. The procedure for the maximization of determinant of the corresponding matrix is proved to be the same as that of the previous QR method in the case of the number of sensors less than that of state variables. On the other hand, the new

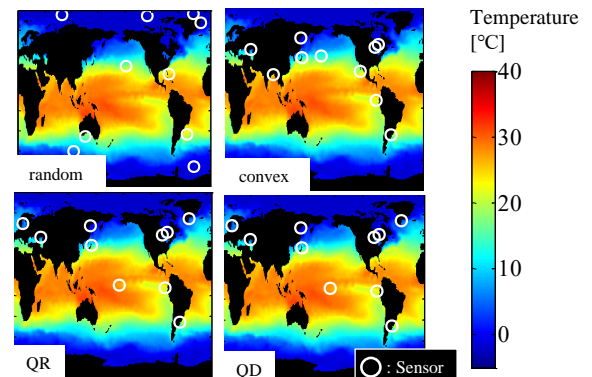


Fig. 6. Sensor positions in $r = p = 10$ for NOAA-SST sensor problem

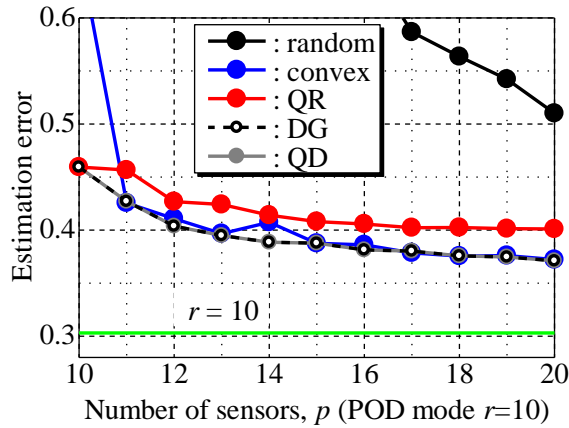


Fig. 7. Estimation error vs. number of sensors in POD mode $r = 10$ for NOAA-SST problem

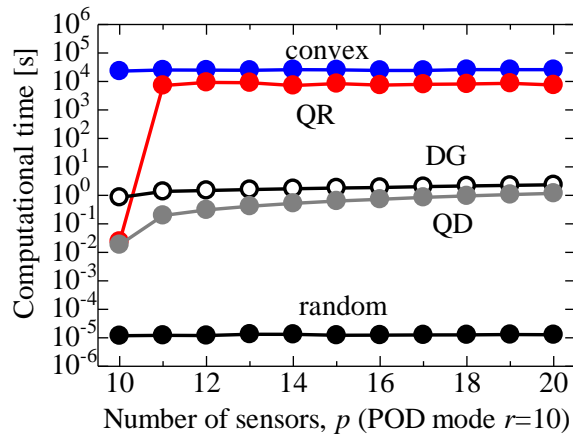


Fig. 8. Computational time vs. number of sensors in POD mode $r = 10$ for NOAA-SST problem

algorithm in the case of the number of sensors greater than that of state variables is developed. The unified formulation is derived, and the lower bound of the objective function given by this algorithm is shown using the monotone submodularity. In the new algorithm, optimal sensors are obtained by the QR method until the number of sensors is equal to state variables, and after that, new sensors are calculated by a proposed determinant-based greedy method which is accelerated by both determinant formula and matrix inversion lemma. The effectiveness of this algorithm on dataset related to global climate dataset is demonstrated by comparing with the results by the other algorithms. The computational time of the proposed extended determinant-based greedy algorithm is shown to be smaller than that of other methods with almost the minimum level of estimation errors. One weakness of the new algorithm is a robustness of noise. The algorithm does not work well for noisy dataset. The improvement of the greedy method will be the subject of challenging future research.

ACKNOWLEDGMENTS

The second author T.N. is grateful for support of the grant JPMJPR1678 of JST Presto.



Yuji Saito received the B.S. degree in mechanical engineering, and the Ph.D. degree in mechanical space engineering from Hokkaido University, Sapporo, Japan in 2018. He is an Assistant Professor of Aerospace Engineering at Tohoku University, Sendai, Japan.



Taku Nonomura received the B.S. degree in mechanical and aerospace engineering from Nagoya University, Nagoya, Japan in 2003, and the Ph. D. degree in aerospace engineering from the University of Tokyo, Tokyo, Japan in 2008. He is currently an Associate Professor of Aerospace Engineering at Tohoku University, Sendai, Japan.



Keigo Yamada received the B.S. degree in physics from Tohoku University, Sendai, Japan, in 2019. He is a M.S. student of engineering at Tohoku University.



Keisuke Asai received the bachelor degree in aeronautical engineering from Kyoto University, Japan, in 1980, and the Ph.D. degree from the University of Tokyo in 1995. He worked at the National Aerospace Laboratory (now, Aeronautical Directorate of JAXA) from 1980 to 2003. He is currently a Professor of Aerospace Engineering at Tohoku University, Sendai, Japan..



Yasuo Sasaki received the B.S. degree from Nagoya University, Nagoya, Japan in 2016. He is currently a Ph.D. student of engineering at Nagoya University.



Daisuke Tsubakino received the B.S. degree from Nagoya University, Nagoya, Japan in 2005 and the Ph.D. degrees in information science and technology from the University of Tokyo, Tokyo, Japan 2011. He is currently a lecturer at Nagoya University.

REFERENCES

- [1] G. Berkooz, P. Holmes, and L. J. Lumley, "The proper orthogonal decomposition in the analysis of turbulent flows," *Annual Review of Fluid Mechanics*, vol. 25, no. 1971, pp. 539–575, 1993.
- [2] K. Taira, S. L. Brunton, S. T. Dawson, C. W. Rowley, T. Colonius, B. J. McKeon, O. T. Schmidt, S. Gordeyev, V. Theofilis, and L. S. Ukeiley, "Modal analysis of fluid flows: An overview," *AIAA Journal*, pp. 4013–4041, 2017.
- [3] P. J. Schmid, "Dynamic mode decomposition of numerical and experimental data," *Journal of Fluid Mechanics*, vol. 656, no. July 2010, pp. 5–28, 2010.
- [4] J. N. Kutz, S. L. Brunton, B. W. Brunton, and J. L. Proctor, *Dynamic mode decomposition: data-driven modeling of complex systems*. SIAM, 2016, vol. 149.
- [5] T. Nonomura, H. Shibata, and R. Takaki, "Dynamic mode decomposition using a kalman filter for parameter estimation," *AIP Advances*, vol. 8, p. 105106, 2018.
- [6] —, "Extended-kalman-filter-based dynamic mode decomposition for simultaneous system identification and denoising," *PLoS one*, vol. 14, p. e0209836, 2019.
- [7] K. Manohar, B. W. Brunton, J. N. Kutz, and S. L. Brunton, "Data-driven sparse sensor placement for reconstruction: Demonstrating the benefits of exploiting known patterns," *IEEE Control Systems Magazine*, vol. 38, no. 3, pp. 63–86, June 2018.
- [8] E. Clark, T. Askham, S. L. Brunton, and J. N. Kutz, "Greedy sensor placement with cost constraints," *IEEE Sensors Journal*, vol. 19, no. 7, pp. 2642–2656, 2018.
- [9] K. Manohar, E. Kaiser, S. L. Brunton, and J. N. Kutz, "Optimized sampling for multiscale dynamics," *Multiscale Modeling & Simulation*, vol. 17, no. 1, pp. 117–136, 2019.
- [10] Y. Saito, T. Nonomura, K. Nankai, K. Asai, Y. Sasaki, and D. Tsubakino, "Data-driven vector-measurement-sensor selection based on greedy algorithm for particle-image-velocimetry measurement," *arXiv preprint arXiv:1906.00778*, 2019.
- [11] S. Chaturantabut and D. C. Sorensen, "Nonlinear model reduction via discrete empirical interpolation," *SIAM Journal on Scientific Computing*, vol. 32, no. 5, pp. 2737–2764, 2010.
- [12] Z. Drmac and S. Gugercin, "A new selection operator for the discrete empirical interpolation method—improved a priori error bound and extensions," *SIAM Journal on Scientific Computing*, vol. 38, no. 2, pp. A631–A648, 2016.
- [13] S. Boyd and L. Vandenberghe, *Convex optimization*. Cambridge University Press, 2004.
- [14] S. Joshi and S. Boyd, "Sensor selection via convex optimization," *IEEE Transactions on Signal Processing*, vol. 57, no. 2, pp. 451–462, 2009.
- [15] R. A. Horn and C. R. Johnson, *Matrix Analysis*, 2nd ed. New York, NY, USA: Cambridge University Press, 2012.
- [16] G. L. Nemhauser, L. A. Wolsey, and M. L. Fisher, "An analysis of approximations for maximizing submodular set functions," *Mathematical programming*, vol. 14, no. 1, pp. 265–294, 1978.
- [17] Y. Saito, K. Yamada, T. Nonomura, K. Asai, D. Tsubakino, and Y. Sasaki, "Code supplement to determinant-based fast greedy sensor selection algorithm," December 2019. [Online]. Available: <https://github.com/YujiSaitoJapan/Determinant-based-Fast-Greedy-Sensor-Selection-Algorithm>
- [18] NOAA/OAR/ESRL, "Noaa optimal interpolation (oi) sea surface temperature (sst) v2," Boulder CO, July 2019. [Online]. Available: <https://www.esrl.noaa.gov/psd/>

APPENDIX

A. *Equivalence for operations of QR and the present method in the case of $k \leq r$*

Theorem A.1. *The QR method is the mathematically equivalent algorithm to the DG method in the case of $k \leq r$.*

Proof: We show the following equality:

$$\mathbf{v}_i \mathbf{v}_i^T = \mathbf{u}_i \left(\mathbf{I} - \mathbf{C}_{k-1}^T (\mathbf{C}_{k-1} \mathbf{C}_{k-1}^T)^{-1} \mathbf{C}_{k-1} \right) \mathbf{u}_i^T \quad (22)$$

in the k th step of OR and DG. Here, \mathbf{v}_i is expressed by \mathbf{u}_i :

$$\mathbf{v}_i = \mathbf{u}_i \mathbf{P}_{k-1}^{\text{QR}}, \quad (23)$$

where $\mathbf{P}_{k-1}^{\text{QR}}$ is the projection matrix corresponding to the Gram-Schmidt operator used in Alg. 1. The squared norm of \mathbf{v}_i of the left-hand side of (22) can be expressed:

$$\mathbf{v}_i \mathbf{v}_i^T = \mathbf{u}_i \mathbf{P}_{k-1}^{\text{QR}} \mathbf{u}_i^T. \quad (24)$$

On the other hand, the right-hand side of (22) can be expressed:

$$\mathbf{u}_i \left(\mathbf{I} - \mathbf{C}_{k-1}^T (\mathbf{C}_{k-1} \mathbf{C}_{k-1}^T)^{-1} \mathbf{C}_{k-1} \right) \mathbf{u}_i^T = \mathbf{u}_i \mathbf{P}_{k-1}^\perp \mathbf{u}_i^T, \quad (25)$$

where $\mathbf{P}_{k-1}^\perp = \left(\mathbf{I} - \mathbf{C}_{k-1}^T (\mathbf{C}_{k-1} \mathbf{C}_{k-1}^T)^{-1} \mathbf{C}_{k-1} \right)$.

Now, we prove the following equation

$$\mathbf{P}_{k-1}^{\text{QR}} = \mathbf{P}_{k-1}^\perp, \quad (26)$$

and the equivalence of operations of the QR and present methods in the case of $k \leq r$ expressed in (22).

The equations in the case of $k = 1$ are written as

$$\mathbf{P}_0^{\text{QR}} = \mathbf{P}_{C_0}^\perp = \mathbf{P}_0^\perp = \mathbf{I}, \quad (27)$$

because both algorithms select the first sensor based on maximizing the norm of the corresponding row vector of \mathbf{U} . The equations in the case of $k = 2$ are expressed as:

$$\mathbf{P}_1^{\text{QR}} = \mathbf{I} - \frac{\mathbf{w}_1^T \mathbf{w}_1}{\|\mathbf{w}_1\|_2^2}, \quad (28)$$

and

$$\begin{aligned} \mathbf{P}_{C_1}^\perp &= \mathbf{I} - \mathbf{C}_1^T (\mathbf{C}_1 \mathbf{C}_1^T)^{-1} \mathbf{C}_1 \\ &= \mathbf{I} - \mathbf{w}_1^T (\mathbf{w}_1 \mathbf{w}_1^T)^{-1} \mathbf{w}_1 \\ &= \mathbf{I} - \frac{\mathbf{w}_1^T \mathbf{w}_1}{\|\mathbf{w}_1\|_2^2}. \end{aligned} \quad (29)$$

Therefore, $\mathbf{P}_1^{\text{QR}} = \mathbf{P}_{C_1}^\perp$ in (28) and (29).

Now, we assume that

$$\mathbf{P}_{k-1}^{\text{QR}} = \mathbf{P}_{k-1}^\perp = \mathbf{P}_{C_{k-1}}^\perp. \quad (30)$$

The equations in the case of $k + 1$ are expressed as:

$$\begin{aligned}
\mathbf{P}_k^{\text{QR}} &= \\
&\left(\mathbf{I} - \frac{\mathbf{w}_1^T \mathbf{w}_1}{\|\mathbf{w}_1\|_2^2} \right) \left(\mathbf{I} - \frac{\mathbf{w}_2^T \mathbf{w}_2}{\|\mathbf{w}_2\|_2^2} \right) \cdots \left(\mathbf{I} - \frac{\mathbf{w}_{k-1}^T \mathbf{w}_{k-1}}{\|\mathbf{w}_{k-1}\|_2^2} \right) \left(\mathbf{I} - \frac{\mathbf{w}_k^T \mathbf{w}_k}{\|\mathbf{w}_k\|_2^2} \right) \\
&= \mathbf{P}_{k-1}^{\text{QR}} \left(\mathbf{I} - \frac{\mathbf{w}_k^T \mathbf{w}_k}{\|\mathbf{w}_k\|_2^2} \right) \\
&= \mathbf{P}_{k-1} \left(\mathbf{I} - \frac{\mathbf{w}_k^T \mathbf{w}_k}{\|\mathbf{w}_k\|_2^2} \right), \tag{31}
\end{aligned}$$

$$\begin{aligned}
\mathbf{P}_{\mathbf{C}_k}^\perp &= \mathbf{I} - \mathbf{C}_k^T (\mathbf{C}_k \mathbf{C}_k^T)^{-1} \mathbf{C}_k \\
&= \mathbf{I} - \begin{pmatrix} \mathbf{C}_{k-1}^T & \mathbf{u}_i^T \end{pmatrix} (\mathbf{C}_k \mathbf{C}_k^T)^{-1} \begin{pmatrix} \mathbf{C}_{k-1}^T \\ \mathbf{u}_i^T \end{pmatrix} \\
&= \left(\mathbf{I} - \mathbf{C}_{k-1}^T (\mathbf{C}_{k-1} \mathbf{C}_{k-1}^T)^{-1} \mathbf{C}_{k-1} \right) \left(\mathbf{I} - \frac{\mathbf{P}_{k-1}^T \mathbf{u}_i^T \mathbf{u}_i \mathbf{P}_{k-1}}{\mathbf{u}_i \mathbf{P}_{k-1} \mathbf{P}_{k-1}^T \mathbf{u}_i^T} \right) \\
&= \mathbf{P}_{k-1} \left(\mathbf{I} - \frac{\mathbf{P}_{k-1}^T \mathbf{u}_i^T \mathbf{u}_i \mathbf{P}_{k-1}}{\mathbf{u}_i \mathbf{P}_{k-1} \mathbf{P}_{k-1}^T \mathbf{u}_i^T} \right). \tag{32}
\end{aligned}$$

See in Appendix B for detailed derivation. Here,

$$\mathbf{w}_k = \mathbf{u}_i \mathbf{P}_{k-1}, \tag{33}$$

$$\mathbf{P}_{\mathbf{C}_k}^\perp = \mathbf{P}_{k-1} \left(\mathbf{I} - \frac{\mathbf{w}_k^T \mathbf{w}_k}{\|\mathbf{w}_k\|_2^2} \right). \tag{34}$$

Assuming sensors selected up to k are the same, the projection matrices for selecting the $(k + 1)$ th sensor are equal to each other, and the row norms calculated at the $(k + 1)$ th time step are the same as each other from (31) and (34). Therefore, the equivalence of operations of QR and DG is proved in the case of the number of sensors: $1 \leq k \leq r$. ■

B. Derivation of $\mathbf{P}_{\mathbf{C}_{k+1}}^\perp$

$$\begin{aligned}
\mathbf{P}_{\mathbf{C}_k}^\perp &= \mathbf{I} - \mathbf{C}_k^T (\mathbf{C}_k \mathbf{C}_k^T)^{-1} \mathbf{C}_k \\
&= \mathbf{I} - \begin{bmatrix} \mathbf{C}_{k-1}^T & \mathbf{u}_i^T \end{bmatrix} \begin{pmatrix} (\mathbf{C}_{k-1} \mathbf{C}_{k-1}^T)^{-1} & \mathbf{0} \\ \mathbf{0} & \mathbf{0} \end{pmatrix} \begin{bmatrix} \mathbf{C}_{k-1} \\ \mathbf{u}_i \end{bmatrix} \\
&\quad - \frac{1}{\mathbf{u}_i \mathbf{P}_{k-1} \mathbf{u}_i^T} \begin{bmatrix} \mathbf{C}_{k-1}^T & \mathbf{u}_i^T \end{bmatrix} \begin{pmatrix} (\mathbf{C}_{k-1} \mathbf{C}_{k-1}^T)^{-1} \mathbf{C}_{k-1} \mathbf{u}_i^T \mathbf{u}_i \mathbf{C}_{k-1}^T (\mathbf{C}_{k-1} \mathbf{C}_{k-1}^T)^{-1} & -(\mathbf{C}_{k-1} \mathbf{C}_{k-1}^T)^{-1} \mathbf{C}_{k-1} \mathbf{u}_i^T \\ -\mathbf{u}_i \mathbf{C}_{k-1}^T (\mathbf{C}_{k-1} \mathbf{C}_{k-1}^T)^{-1} & 1 \end{pmatrix} \begin{bmatrix} \mathbf{C}_{k-1} \\ \mathbf{u}_i \end{bmatrix} \\
&= \mathbf{I} - \mathbf{C}_{k-1}^T (\mathbf{C}_{k-1} \mathbf{C}_{k-1}^T)^{-1} \mathbf{C}_{k-1} - \frac{1}{\mathbf{u}_i \mathbf{P}_{k-1} \mathbf{u}_i^T} \left(\mathbf{C}_{k-1}^T (\mathbf{C}_{k-1} \mathbf{C}_{k-1}^T)^{-1} \mathbf{C}_{k-1} \mathbf{u}_i^T \mathbf{u}_i \mathbf{C}_{k-1}^T (\mathbf{C}_{k-1} \mathbf{C}_{k-1}^T)^{-1} \mathbf{C}_{k-1} \right. \\
&\quad \left. - \mathbf{C}_{k-1}^T (\mathbf{C}_{k-1} \mathbf{C}_{k-1}^T)^{-1} \mathbf{C}_{k-1} \mathbf{u}_i^T \mathbf{u}_i - \mathbf{u}_i^T \mathbf{u}_i \mathbf{C}_{k-1}^T (\mathbf{C}_{k-1} \mathbf{C}_{k-1}^T)^{-1} \mathbf{C}_{k-1} + \mathbf{u}_i^T \mathbf{u}_i \right) \\
&= \mathbf{I} - \mathbf{C}_{k-1}^T (\mathbf{C}_{k-1} \mathbf{C}_{k-1}^T)^{-1} \mathbf{C}_{k-1} - \frac{\mathbf{I} - \mathbf{C}_{k-1}^T (\mathbf{C}_{k-1} \mathbf{C}_{k-1}^T)^{-1} \mathbf{C}_{k-1}}{\mathbf{u}_i \mathbf{P}_{k-1} \mathbf{u}_i^T} \left(\mathbf{u}_i^T \mathbf{u}_i \left(\mathbf{I} - \left(\mathbf{C}_{k-1}^T (\mathbf{C}_{k-1} \mathbf{C}_{k-1}^T)^{-1} \mathbf{C}_{k-1} \right) \right) \right) \\
&= \mathbf{P}_{k-1} - \frac{\mathbf{P}_{k-1}}{\mathbf{u}_i \mathbf{P}_{k-1} \mathbf{u}_i^T} \left(\mathbf{u}_i^T \mathbf{u}_i \mathbf{P}_{k-1} \right) \\
&= \mathbf{P}_{k-1} \left(\mathbf{I} - \frac{\mathbf{u}_i^T \mathbf{u}_i \mathbf{P}_{k-1}}{\mathbf{u}_i \mathbf{P}_{k-1} \mathbf{u}_i^T} \right) \\
&= \mathbf{P}_{\mathbf{C}_{k-1}} \left(\mathbf{I} - \frac{\mathbf{P}_{k-1} \mathbf{u}_i^T \mathbf{u}_i \mathbf{P}_{k-1}}{\mathbf{u}_i \mathbf{P}_{k-1} \mathbf{u}_i^T} \right) \tag{35}
\end{aligned}$$